Reprinted from JOURNAL OF APPLIED PHYSICS, Vol. 38, No. 6, 2599–2605, May 1967

Stability of an Electrified Liquid Jet*

J. M. SCHNEIDER,† N. R. LINDBLAD, C. D. HENDRICKS, JR., AND J. M. CROWLEY
Department of Electrical Engineering, University of Illinois, Urbana, Illinois
(Received 30 August 1966; in final form 9 December 1966)

A capillary wave of the appropriate wavelength will cause a jet to break up into a stream of uniform-sized droplets. In this paper, a theoretical expression for droplet size, radius, and spacing in terms of the jet parameters and applied frequency is derived and verified experimentally. For a given jet radius and velocity, the droplet size can be varied from its minimum value, r_{min}, to approximately $1.6r_{min}$ by varying the driving frequency. Also, a theoretical expression for the charge on droplets resulting from the disintegration of a charged jet is shown to agree with the measured value of droplet charge.

I. INTRODUCTION

The breakup of a charged liquid jet has been studied by several authors in the last century.[1,2] In most of this work, the response of the jet to small sinusoidal perturbations of the surface has been analyzed to find the wavelengths or frequencies at which the disturbance will grow, eventually causing breakup of the jet. Very little work, however, has been done on the nature of the droplets produced by this breakup process.

In this paper, we will study, theoretically and experimentally, the radius, velocity, spacing, and charge of these droplets in terms of the properties of the jet and the applied electric field. The appendix contains a new derivation of the dispersion relation for a charged jet, based on Rayleigh's[3] technique.

II. EXPERIMENTAL APPARATUS

The droplet generator,[4–6] shown in Fig. 1, produces a stream of uniform-sized droplets. The liquid jet is formed by forcing liquid under pressure through a small glass capillary. Attached to the capillary is a piezoelectric transducer which excites a transverse and an axial wave on the jet. The jet first exhibits a snaking mode which couples into a bulging mode as shown in Fig. 2. The growth of this bulging mode due to surface tension then causes the breakup of the jet into uniform droplets. In this photograph the jet diameter was 63.3 μ and its length was approximately 1.5 mm.

In the electrical apparatus, also shown in Fig. 1, the signal from the oscillator is amplified to furnish the necessary voltage for the transducer. To produce charged droplets a variable dc-power supply applies a steady potential between the jet and the charging electrode. The charge on the droplets is determined by directing the stream into a nearly closed container, measuring the current between the container and ground with a micromicroammeter. If the potential on the jet is kept constant, then all the droplets are similarly charged and the charge per droplet is given by the current divided by the number of droplets per unit time (i.e., the driving frequency). The accuracy in measuring the droplet charge is determined by the accuracy of the micromicroammeter which is within 4%.

In the calculations involving charging of droplets by this method it is assumed that the conductivity of the liquid is so high that charge relaxation occurs much faster than the time needed for a point in the jet to move through the charging electrode. All the results in this paper pertain to distilled water, which has a conductivity of 2×10^{-4} mhos/m, corresponding to relaxation time of approximately 3.5 μsec. The time for a particle of the jet to move through the charging electrode of length 1.27 cm is approximately 2.1 msec for a jet velocity of 600 cm/sec. Hence, the charge relaxation time for water is approximately three orders of magnitude less than the mechanical-time constant for the jet.

III. THE BREAKUP OF THE JET

The previous section describes how the jet, which is excited at a steady frequency f, breaks up into droplets under the influence of the surface tension. In this section we shall attempt to find the radius, velocity, and spacing of these droplets.

In each cycle of the driving frequency, more than one droplet may be created as a result of nonlinearities in the exciter or in the fluid motion which produce harmonics of the driving frequency. If any of these harmonic frequencies correspond to unstable disturbances, two or more unstable wavelengths will grow on the jet, producing several satellite droplets in every cycle. These satellite droplets may spray off at an angle with respect to the main stream or follow directly behind the main droplets. Those following directly behind eventually overtake the parent droplet and coalesce with it. The satellites can usually be eliminated by a slight adjustment of either the frequency or the voltage

* This research supported by the Section on Atmospheric Sciences, National Science Foundation, NSF Grant GP-5487 and Department of Health, Education, and Welfare, PHS Grant AP-00511-01.
† Present Address: Xerox Corporation; Rochester, New York, 14603.
[1] A. B. Basset, Am. J. Math. **16,** 93 (1894).
[2] J. R. Melcher, *Field-Coupled Surface Waves* (The M.I.T. Press, Cambridge, Massachusetts, 1963), Chap. 6.
[3] Lord Rayleigh, Proc. London Math. Soc. **10,** 4 (1878).
[4] J. M. Schneider and C. D. Hendricks, Jr., Rev. Sci. Instr. **35,** 1349 (1964).
[5] N. R. Lindblad and J. M. Schneider, J. Sci. Instr. **42,** 635 (1965).
[6] J. M. Schneider, N. R. Lindblad, and C. D. Hendricks, Jr., J. Colloid Sci. **20,** 610 (1965).

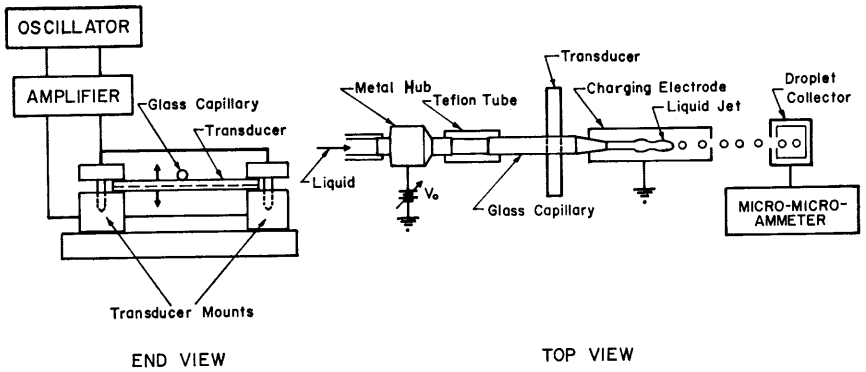

FIG. 1. Schematic diagram of the experimental apparatus.

applied to the transducer. They will be neglected in the discussion which follows. With this restriction, the radius of the jet at every point will be periodic, with minima occurring f times every second. At that point where the minimum radius is zero, a droplet will break off from the jet f times every second (once in every cycle).

Most of the properties of the droplets result from the conservation of mass and momentum during the breakup process. The jet enters the closed volume shown in Fig. 3 with an infinitesimal disturbance which does not affect the mass or momentum. Inside the box, the jet breaks up into spherical droplets of radius, r_d, which leave with a velocity, v_d, and a center to center spacing, d. Conservation of mass then states that

$$\pi a^2 v_J = 4\pi r_d^3 v_d/3d, \tag{1}$$

where v_J is the jet velocity. The conservation of momentum, neglecting viscosity, gives

$$\eta\pi a^2 v_J^2 = 4\eta\pi r_d^3 v_d^2/3d + \pi a T, \tag{2}$$

where T is the surface tension of the liquid and η is the density.

Solution of these two equations gives the radius as

$$r_d = (3a^2 d v_J/4v_d)^{1/3} = (3a^2 v_J/4f)^{1/3}, \tag{3}$$

where f is the driving frequency. The velocity of the drop is

$$v_d = v_J'(1 - v_c^2/v_J^2), \tag{4}$$

where v_c is the velocity of capillary waves on the jet,

$$v_c^2 = T/\eta a. \tag{5}$$

Interestingly enough, the drop velocity is not directly related to the propagation velocity for disturbances on the jet. Thus, although we think of each cycle of the disturbance growing into a single droplet, the velocity of this droplet is determined only by the conservation laws.

The separation between droplets results from the kinematics of the droplet stream. If f drops are formed every second, and they travel with a velocity, v_d, the separation between them is

$$d = v_d/f, \quad \text{or} \quad fd/v_J = (1 - v_c^2/v_J^2). \tag{6}$$

The normalized-droplet separation, fd/v_J, is plotted in Fig. 4, along with experimentally measured points. In this measurement, the droplet spacing and jet radius were measured with a microscope reticule. The frequency was determined with an electronic counter, while the mass-flow rate and jet radius supplied the jet velocity. For each velocity (or mass-flow rate), the droplet spacing was measured for at least six different frequencies. The values of fd/v_J obtained, which showed a total spread of about 3%, were averaged to obtnia the experimental points shown in the figure.

The graph shows that the spacing is given very closely by

$$d = v_J/f, \tag{7}$$

when the square of the jet velocity is much larger than the square of the capillary velocity. In the remainder of the experimental work described here, the ratio $(v_J/v_c)^2 \geq 9$, so the approximation should be valid.

The curve of driving frequency vs. droplet radius (Fig. 5) shows that the radius of the droplet, measured

FIG. 2. Photograph of a perturbed jet to show transverse and axial waves.

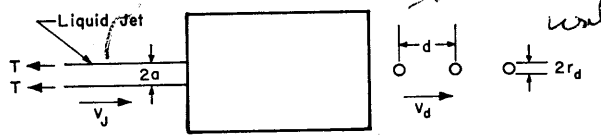

FIG. 3. A system sketch to illustrate the conservation of mass and momentum.

with a microscope reticule, agrees with that predicted by conservation of mass [Eq. (1)].

At frequencies outside the range shown in Fig. 5, it was not possible to produce a uniform beam of droplets. Rayleigh[3] has shown that the lower limit of the droplet radius corresponds closely to a wavelength slightly greater than the circumference of the jet, which agrees with results shown in Fig. 5. His theory, however, does not predict an upper limit on the droplet size since there is no lower limit on the frequency at which the jet is unstable. Thus, arbitrarily large droplets appear possible. To examine this possibility consider Eq. (A1) In this equation the coefficient, c, is proportional to $e^{\omega t}$ where the value of ω determines the manner in which the liquid departs from its circular cylindrical shape for a disturbance of wavelength, λ. The larger the value of ω, the smaller the time required for breakup. The value of ω^2 from Eq. (A3), neglecting electrical effects, is

$$\omega^2 = T(1-n^2a^2)maI_1(ma)/\eta a^3 I_0(ma),$$

where $I_0(ma)$ and $I_1(ma)$ are modified Bessel functions of zero and first order. A plot of $\omega^2\eta a^3/T$ as a function of $\lambda/2\pi a$, shown in Fig. 6, indicates the wavelengths which are most influential in producing the instability. The peak located at $\lambda=1.43(2\pi a)$ yields the wavelength which produces the most rapid instability, that is, $\lambda=9a$. This figure shows that the rate at which instability grows is very low at the longer wavelengths. Thus if the driver excites a low frequency, the growth of this disturbance could be so slow that noise near the optimum wavelength is amplified to cause breakup while the driven disturbance is still small. For the experimental results shown here, the upper limit on wavelength is about $36a$. Thus the wavelength, λ,

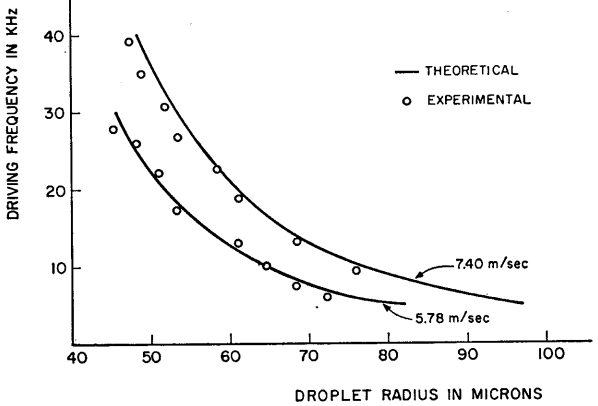

FIG. 5. Driving frequency vs droplet radius for water jet moving at 5.78 m/sec and 7.40 m/sec.

which causes breakup can be varied between the approximate limits

$$7a<\lambda<36a.$$

This corresponds to varying the droplet radius from $r_{\min}$ to approximately $1.6r_{\min}$ for a given-size jet. It may be possible to extend the range of λ and r_d upward by reducing the noise on the jet.

IV. THE CHARGE ON THE DROPLETS

The net charge on the droplet produced at the end of the jet determines its motion in an electric field, and must therefore be known for the application of these droplets. Consider first the case in which the liquid conductivity is high enough to allow a steady surface charge to form before the jet breaks up, but not so high that the charge can change appreciably during the breakup. The charge will then be trapped on the

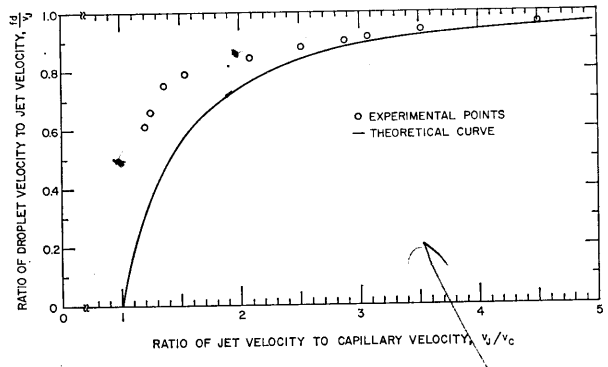

FIG. 4. When the jet velocity, v_j, is near the capillary velocity, v_c, the droplet velocity, v_d, is reduced. At high velocities, the droplet velocity approaches the jet velocity.

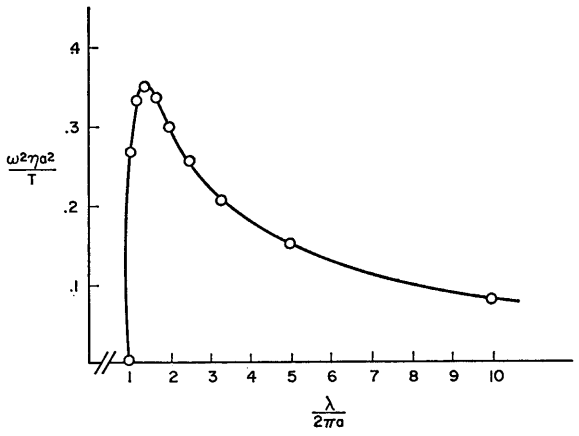

FIG. 6. Jet instability due to charge vs the wavelength divided by the circumference of the jet.

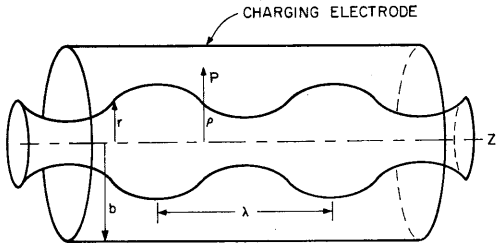

FIG. 7. Diagram of a perturbed jet inside of a charging electrode.

surface, and the net charge on each droplet will be the net charge on the length, l, of the jet which goes into the formation of one drop, namely

$$Q=2\pi\epsilon_0 V_o/\ln(b/a).$$

When the relaxation time of the fluid is shorter than the breakup time, however, the net charge on the drop will be determined in part by the electric field at the surface of the jet when the drop breaks away. Since the determination of the electric field under these conditions would be extremely difficult, we will consider an approximation in which this effect is not important. Consider the geometry shown in Fig. 7, where the jet is surrounded by a grounded cylindrical electrode of radius b. Assume that the jet is charged to a potential, V_o, and that the perturbation on the jet is small so that terms in c^2 can be neglected. Furthermore, it is assumed that the charge located on the jet on any given undulation of wavelength, λ, ultimately becomes the charge on a given droplet, and that the mass of an undulation becomes the mass of a given droplet. (This implies that $v_J^2 \gg v_c^2$, as discussed in Sec. III).

The potential in the region between the jet and the cylindrical charging electrode (both of which are concentric with the Z axis) is composed of two terms. One term is

$$V_C=(V_o \ln\rho/b)/\ln(a/b),$$

which expresses the potential at a radius ρ between two coaxial conductors of inner radius a and outer radius b. The other term is due to the slight perturbation on the inner conductor given by $r=a+c\cos mz$. This potential, V_P, at the point, P, again has no ϕ-dependence and varies as $\cos mz$ along the Z axis, thus

$$V_P=[DI_0(m\rho)+EK_0(m\rho)]\cos mz,$$

so that the complete form of the potential is

$$V=(V_o \ln\rho/b)/\ln(a/b)+[DI_0(m\rho)+EK_0(m\rho)]\cos mz.$$

From the boundary conditions $V=0$ at $\rho=b$ and $V=V_o$ at $\rho=a+c\cos mz$ one obtains

$$E=-DI_0(mb)/K_0(mb),$$

and

$$D=V_o cK_0(mb)/a(\ln a/b)[I_0(ma)K_0(mb)-I_0(mb)K_0(ma)].$$

Thus, the potential in the region between the jet and charging electrode has the form

$$V=\frac{V_o}{\ln a/b}\left\{\ln\rho/b-\frac{c}{a}\left[\frac{I_0(m\rho)K_0(mb)-I_0(mb)K_0(m\rho)}{I_0(ma)K_0(mb)-I_0(mb)K_0(ma)}\right]\cos mz\right\}.$$

The charge, Q, on an undulation or droplet can be calculated from

$$Q=\int_A \sigma dA,$$

where σ is the surface-charge density which is approximately given by

$$\sigma\approx-\epsilon_o(\partial V/\partial\rho)\mid_{\rho=a+c\cos mz}.$$

If the fact that $\dot{K}_0(m\rho)=K_1(m\rho)\approx K_1(ma)$ and $\dot{I}_0(m\rho)=I_1(m\rho)\approx I_1(ma)$ is used, one obtains

$$\sigma=\epsilon_o V_o[1-(c/a)\cos mz-mcI\cos mz]/a\ln a/b,$$

where

$$I=[I_1(ma)K_0(mb)-I_0(mb)K_1(ma)]/[I_0(ma)K_0(mb)-I_0(mb)K_0(ma)].$$

Hence, the charge, Q, in a single undulation is

$$Q=-\frac{2\pi\epsilon_o V_o}{a\ln a/b}\int_{z_0}^{z_0+2\pi/m}(1-(c/a)\cos mz-mcI\cos mz)(a+c\cos mz)dz,$$

or

$$Q=2\pi\epsilon_o V_o\lambda/\ln(b/a) \qquad (8)$$

since $\lambda=2\pi/m$. By using Eq. (7) the wavelength, λ, can be expressed in terms of measurable quantities such as the jet velocity, v_J, and the driving frequency f; thus,

$$Q=2\pi\epsilon_o V_o v_J/f(\ln b/a).$$

Thus, when the jet is highly conducting, a slight perturbation of the surface will not affect the *average* charge per unit length of the jet, which then behaves

exactly like the poorly conducting jet. As the disturbance becomes larger, as it will near the breakup point, this perturbation theory will no longer give a valid description of the surface charge. In the interest of simplicity, however, we assume that the charge of a drop is equal to the charge per wavelength of the perturbation. This assumption must, of course, be verified experimentally.

Figure 8 shows the theoretical and experimental values of droplet charge vs capillary voltage for two different diameters of charging electrode. The theoretical curve for both the large and small electrode are nearly identical. The upper experimental curve (solid line), which agrees very accurately with the theoretical curve for potentials greater than 20 V, was obtained with a small-charging electrode. The length and diameter of this charging electrode were 1.27 cm and 0.29 cm, respectively. The lower experimental curve was obtained with a charging electrode of the same length, but with a slightly larger diameter (0.37 cm). Since the diameter of the jet was 55.2 μ, the ratio, b/a, for the upper and lower curve was approximately 53 and 67, respectively. The discrepancy between calculated and measured values of droplet charge for large electrodes and small potentials is probably due to the influence of fields from various extraneous sources. From these results, it appears that the ratio, b/a, should be kept as small as is practically possible so that the effects of these fields will be minimized. The ratio of the length to radius of the charging electrode is important for the same reason. If it were possible to keep the ratio of length to radius constant, the diameter of the charging electrode might not be as important.

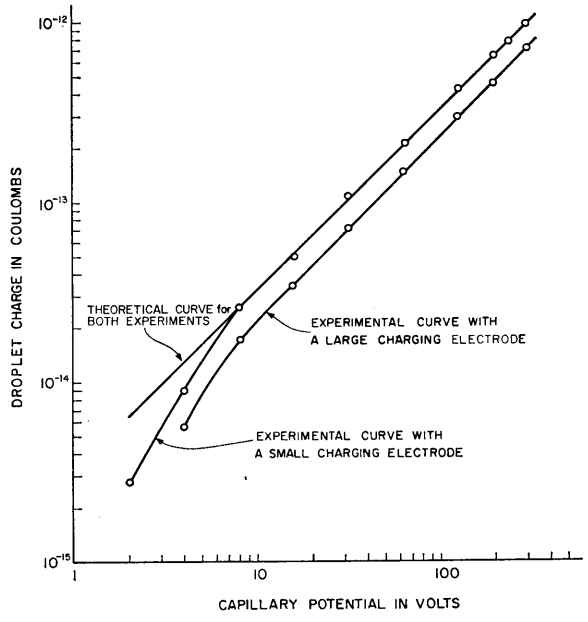

FIG. 8. Charge on water droplets vs capillary potential with a small- and large-charging electrode.

However, the length of the jet places a practical limitation on the length of the charging electrode and therefore the ratio, b/a, is critical.

The charge on the droplet stream was measured by utilizing a micromicroammeter. With this method, the stream of charged droplets was directed into a nearly closed container and the current from the container to ground was measured.

If Eq. (3) is used to eliminate λ from Eq. (8), the specific charge (charge to mass ratio) of the droplets is

$$Q/M = 2\epsilon_0 V_0/a^2\eta \ln(b/a).$$

This equation, which indicates that the specific charge is directly dependent on the potential, is true only for a limited range of potentials because no account has been taken of space-charge conditions. An interesting feature of this result is that the specific charge is independent of the wavelength of the disturbance of the jet because the charge and mass of a wavelength became the charge and mass of the droplet.

V. SUMMARY

The radius, velocity, and spacing of droplets ejected from the end of an unstable jet can be calculated in terms of the jet velocity, radius, and surface tension. When the inertia forces are much larger than the surface-tension forces, the droplet velocity is very nearly equal to the jet velocity, and the radius is given by

$$r_d = (3a^2 v_J/4f)^{1/3}.$$

The charge on the droplet is given approximately by the total charge over one wavelength of that jet perturbation which eventually grows to form one drop, namely

$$Q = 2\pi\epsilon_0 V_0 v_J/f(\ln b/a).$$

The charge to mass ratio is therefore independent of the jet velocity and applied frequency.

APPENDIX I: EXTENSION OF RAYLEIGH'S THEORY FOR CHARGED JETS

Rayleigh, in his analysis of the instability of a liquid jet, did not examine the effect of electric charge on the jet. Basset[1] investigated the instability of a liquid jet in a more general manner by including the velocity, viscosity, surface tension, influence of the surrounding air, and the electric charge on the jet. We shall extend Rayleigh's work by including the effect of electric charge and show that it is in complete agreement with Basset's more detailed study.

In Rayleigh's analysis it is assumed that the jet has the shape illustrated in Fig. A1 where the radius r of the jet at time t can be approximated for small perturbations by the equation,

$$r = a_0 + c\cos mz, \qquad \text{(A1)}$$

where a_0 is not a constant but is constrained by the

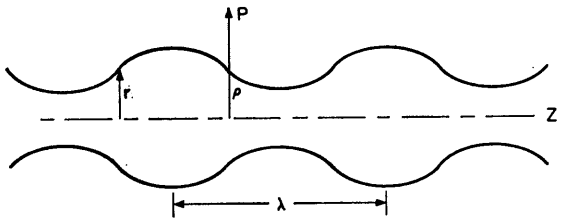

FIG. A1. Diagram of a perturbed jet.

fact that the volume per unit length, V_L, along the jet is a constant, c is a small quantity variable with time, m is the wavenumber $2\pi/\lambda$, where λ is the wavelength of the disturbance, and the cylindrical jet is axially symmetric with respect to the Z coordinate.

When charge is present on the jet, Rayleigh's theory must be modified to take into account the potential energy of the charge. For a perturbed jet axially symmetric with respect to the Z axis as shown in Fig. A1, the potential, V, of a point, P, at a distance, ρ, normal to the axis, is the sum of two potentials: one due to a charged circular cylinder of liquid and the other due to a charged perturbed jet. The potential, V_C, of the circular cylinder of radius, a, is

$$V_C = V_o \ln\rho/\ln a,$$

where V_o is the potential at $\rho = a$. The potential, V_P, of the perturbed jet depends only on ρ and z so that the solution to Laplace's equation has the form

$$V_P = Z(z)\,R(\rho).$$

Since the potential of the perturbed jet varies as $\cos mz$ along the Z axis, we have

$$Z(z) = A\cos mz.$$

In this case, the radial term must be expressed in terms of the modified Bessel function $I_n(m\rho)$ and $K_n(m\rho)$, that is,

$$R(\rho) = BI_n(m\rho) + CK_n(m\rho).$$

Since the potential, V_P, is axially symmetric, $n=0$, so that the expression for V_P becomes

$$V_P = [B'I_0(m\rho) + C'K_0(m\rho)]\cos mz.$$

The function, $I_0(m\rho)$, is finite at $m\rho = 0$ and infinite at $m\rho = \infty$. This makes it unsuitable for the region outside the jet and must be excluded, i.e., $B' = 0$. The function, $K_0(m\rho)$, is infinite at $m\rho = 0$ and zero at $m\rho = \infty$, making it suitable for the region outside the jet. Thus, the potential, V, becomes

$$V = V_o \ln\rho/\ln a + C'K_0(m\rho).$$

To describe the potential of a conducting jet correct to first order in c we let $a_o = a$ in Eq. (A1). Thus, at $\rho = r$, $V = V_o$ we find

$$C' = -cV_o/(a\ln a)K_0(ma),$$

so that

$$V = V_o/\ln a\{\ln\rho - [cK_0(m\rho)/aK_0(ma)]\cos mz\}.$$

This expression for the potential is correct to first order in c and can be used to calculate, approximately, the second-order perturbation in the potential energy per unit length P_L. This energy is one-half the charge per unit length, Q_L, multiplied by the potential of the jet, V_o, that is,

$$P_L = Q_L V_o/2.$$

The charge per unit length on the jet is given by

$$Q_L = \frac{2\pi}{\lambda}\int_0^\lambda \sigma r\,dz,$$

where σ is the surface-charge density which can be calculated from

$$\sigma = -\epsilon_o \partial V/\partial\rho.$$

When σ is evaluated at $r = a + c\cos mz$, the surface-charge density becomes approximately

$$\sigma \approx -\frac{\epsilon_o V_o}{\ln a}\left[a^{-1} - \frac{c}{a^2}\cos mz - \frac{cmK_1(ma)}{aK_0(ma)}\cos mz\right],$$

where the factor $\dot{K}_0 = K_1$ was used. The charge per unit length is

$$Q_L = \frac{2\pi}{\lambda}\int_0^\lambda \sigma r\,dz$$

$$= -\frac{2\pi\epsilon_o V_o}{\ln a}\left[1 - \frac{c^2}{2a^2} - \frac{c^2 mK_1(ma)}{2aK_0(ma)}\right],$$

and the potential energy per unit length is

$$P_L = -\frac{\pi\epsilon_o V_o^2}{\ln a}\left[1 - \frac{c^2}{2a^2} - \frac{c^2 mK_1(ma)}{2aK_0(ma)}\right].$$

The potential energy, P_R, relative to the circular cylinder is

$$P_R = P_L - P_o$$

where P_o is the potential energy per unit length of the unperturbed cylinder of liquid. This energy is

$$P_o = Q_{CL}V_o/2 = -\pi\epsilon_o V_o^2/\ln a$$

where $Q_{CL} = -2\pi\epsilon_o V_o/\ln a$ is the charge per unit length on the unperturbed cylinder. Thus,

$$P_R = \frac{\pi\epsilon_o V_o^2}{2\ln a}\left[1 + \frac{maK_1(ma)}{K_0(ma)}\right]\frac{c^2}{a^2}.$$

The total potential energy, P, relative to the undisturbed cylinder is the sum of the potential energy per unit length due to surface tension and the potential energy per unit length due to charge. The potential energy per unit length, P_T, due to surface tension was calculated by Rayleigh[3] and is

$$P_T = -T\pi c^2(1 - m^2a^2)/2a.$$

Lagrange's method can be used to obtain the time

variation in the quantity, c. Since the Lagrangian is the kinetic energy K minus the potential energy P, the differential equation for a charged jet is

$$\ddot{c}-\frac{T}{\eta a^3}\left[\frac{(1-m^2a^2)maI_1(ma)}{I_0(ma)}\right]c+\frac{\epsilon_0 V_0^2 maI_1(ma)}{\eta a^4(\ln a)I_0(ma)}\left[1+\frac{maK_1(ma)}{K_0(ma)}\right]c=0, \tag{A2}$$

where the expression for the kinetic energy

$$K=\frac{\pi\eta a^2 I_0(ma)}{2maI_1(ma)}\dot{c}^2$$

from Rayleigh's work was used.

If the displacement of the surface is exponential in time, with the growth rate, ω, the differential equation, Eq. (A2), reduces to the dispersion relation.

$$\omega^2=\frac{T}{\eta a^3}\left[\frac{(1-m^2a^2)maI_1(ma)}{I_0(ma)}\right]-\frac{\epsilon_0 V_0^2 maI_1(ma)}{\eta a^4(\ln a)I_0(ma)}\left[1+\frac{maK_1(ma)}{K_0(ma)}\right], \tag{A3}$$

which is valid in the coordinate system attached to the jet. This agrees with the results obtained by Basset[1] and Melcher.[2]

In Eq. (A2) the influence of surface tension on jet stability is illustrated in the second term (first coefficient of c). The third term in this equation arose from the charge on the jet. To examine the effect of charge on the dynamical stability of a liquid jet, a normalized graph of this function vs $\lambda/2\pi a$ is shown in Fig. A2. For wavelengths slightly less than the circumference of the jet, charge promotes instability since $f(ma)$ is negative. For values of $\lambda > 1.66$ times the circumference, $f(ma)$ is positive, indicating that charge promoted stability.

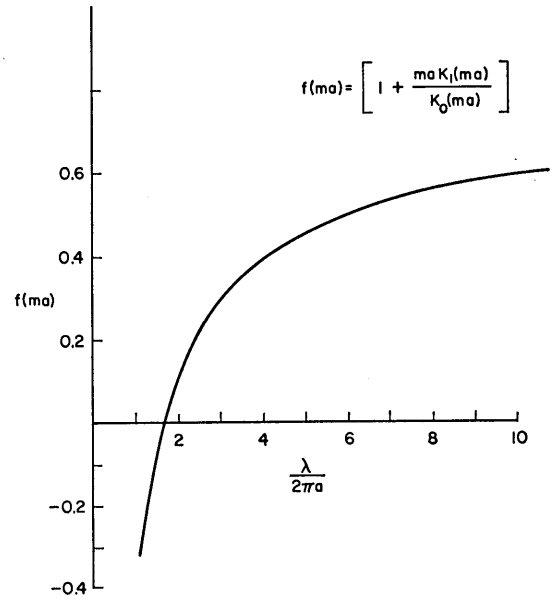

FIG. A2. Jet stability due to charge vs the wavelength divided by the circumference of the jet.

Since a practical jet is frequently in the region where charge promotes stability, it is of interest to compare the two coefficients of c in Eq. (A2). A plot of the first coefficient of c, f_T and the second coefficient of c, f_C is shown in Fig. A3. The charge term is only important for wavelengths slightly greater than the circumference of the jet. Since the usual mode of operation for producing uniform-sized droplets is between $7a<\lambda<36a$, the importance of charge on the jet instability is negligible compared to the effect of surface tension. The values of V_0 and jet radius used in this figure were 100 V and 25 μ. This potential corresponds very closely to the maximum charge per unit length that can be retained in air by a cylindrical column of liquid 25 μ in radius. Thus, the graph of f_C in Fig. A3 is for a highly charged jet.

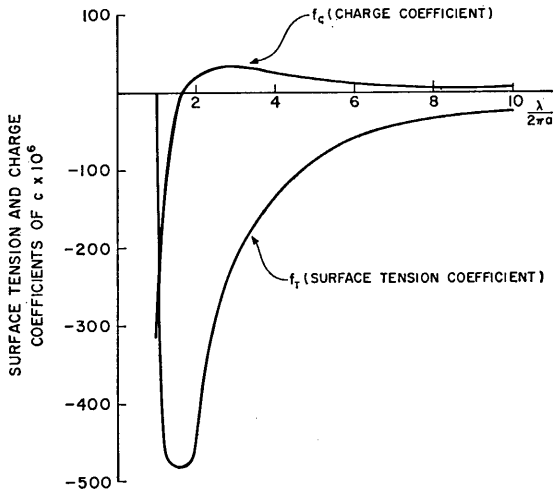

FIG. A3. The coefficients of c due to surface tension and charge vs the wavelength divided by the circumference of the jet.